DALTON
FULL PAPER

Spin distribution in copper(I) phosphine complexes of verdazyl radicals †

David J. R. Brook * and Vincent Abeyta

Department of Chemistry and Biochemistry, University of Detroit Mercy, P.O. Box 19900, Detroit, MI 48219-0900, USA

Received 19th June 2002, Accepted 9th September 2002
First published as an Advance Article on the web 21st October 2002

Copper(I) forms mixed ligand coordination compounds with the stable, paramagnetic bipyridine analogue, 1,5-dimethyl-3-(2-pyridyl)-6-oxoverdazyl (pyvd) and a variety of monodentate and bidentate phosphine ligands. These compounds were characterized in solution by titration, UV-vis spectra, ESR spectra and electrospray mass spectrometry. Coordination of the phosphine gives a metal–ligand charge transfer transition in the UV-vis that is red shifted by more electron donating phosphines. ESR indicates that spin density on copper increases, both with strongly electron donating phosphines and with weakly basic phosphite ligands. This can be explained by the presence of two different orbital interactions: with more donating phosphines the interaction is predominantly through the filled copper(I) d-orbitals, but with weakly donating phosphite ligands the interaction is through an empty copper(I) p-orbital. The differing spin transfer mechanisms may have implications in the design of molecular magnetic systems.

Introduction

Various methods have been proposed for the synthesis of extended molecules and materials with bulk magnetic properties. One of the most productive has been the linking of transition metal ions with bridging radical ligands. Typically, the radical ligands have been nitronyl nitroxides, but a variety of other free radicals have also been investigated, among them the 6-oxoverdazyls.[1–4] These heterocyclic radicals are of particular interest because of their structural resemblance to pyrimidines. Pyrimidines and other heterocyclic amine ligands have been extensively used to form large self assembled systems[5–14] suggesting the possibility of similar structural design with paramagnetic systems. Our initial studies of the coordination chemistry of the 1,1′,5,5′-tetramethyl-6,6′-dioxo-3,3′-biverdazyl (bvd) indicated that the interaction between the two radical centers was strongly perturbed by the coordination of copper(I).[2] Furthermore we speculated that the extent of interaction through the copper(I) ion would be modulated by the nature of the ancillary ligands on copper. Computational studies by Green and co-workers have subsequently supported this idea.[15] This contrasts with recently published work where the interaction between two verdazyls mediated by copper(I) was very small (≈2 cm^{-1}).[16] In order to further probe the copper(I)–verdazyl interaction and in particular, the role of ancillary ligands, we have been studying the coordination chemistry of the chelating monoverdazyl 1,5-dimethyl-3-(2-pyridyl)-6-oxoverdazyl (pyvd). Initial studies demonstrated the coordination of copper(I) bromide analogously to bvd;[1] however interaction between free radicals hindered the spin distribution study. In this work, by using a variety of phosphine ancillary ligands, we have been able to generate a series of copper–phosphine–verdazyl complexes and characterize these species in solution by ESR, UV-vis spectroscopy and mass spectrometry (Scheme 1).

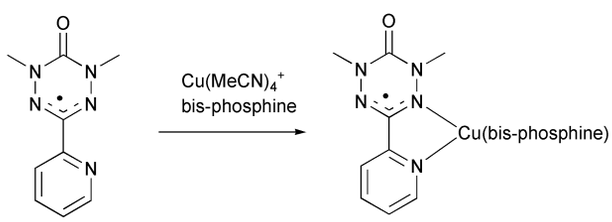

bis-phosphine=$(Ph_3P)_2$, $[(p\text{-tolyl})_3P]_2$, $[(PhO)_3P]_2$, dppe, dppp, dppb, dppf, xantphos

Scheme 1

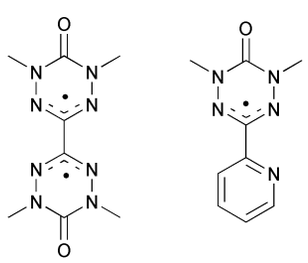

bvd **pyvd**

Experimental

General

1,5-Dimethyl-3-(2-pyridyl)-6-oxoverdazyl (pyvd) was synthesized as previously described[20] and stored under liquid nitrogen. 4,5-Bis(diphenylphosphino)-9,9-dimethylxanthene (xantphos) was synthesized *via* published procedures.[17] Triphenylphosphine, tri-*p*-tolylphosphine, triphenyl phosphite, 1,2-bis(diphenylphosphino)ethane (dppe), 1,3-bis(diphenylphosphino)propane (dppp), 1,4-bis(diphenylphosphino)butane (dppb), 1,1′-bis(diphenylphosphino)ferrocene (dppf) and tetrakis(acetonitrile)copper(I) hexafluorophosphate were purchased from commercial suppliers and used as received. ESR spectra were recorded on a Bruker ESP300e X band

† Electronic supplementary information (ESI) available: ESR spectra. See http://www.rsc.org/suppdata/dt/b2/b205923c/

spectrometer at 300 K and simulated with the program Winsim.[18] Electrospray mass spectra were recorded on an Agilent 1100 SL ion trap mass spectrometer.

Titrations

Solutions of pyvd in dichloromethane were quantified by UV-vis spectroscopy. A solution of one equivalent of $Cu(MeCN)_4^+PF_6^-$ was added to give a solution of 'Cu(pyvd)$^+$'. The stirred solution was then titrated with a solution of phosphine by means of a calibrated syringe pump. UV-spectra of the solution were recorded at regular intervals with an Ocean Optics PC2000 diode array spectrophotometer. UV-vis spectral data were analyzed with MATLAB®.[19]

Results

When solutions of Cu(I) and pyvd are titrated with solutions of monodentate (triphenylphosphine, tri-*p*-tolylphosphine and triphenyl phosphite) and bidentate (dppe, dppp, dppb, dppf and xantphos) phosphines, distinct spectral changes are observed. With monodentate phosphines two well defined end points are observed corresponding to phosphine : copper ratios of 1 : 1 and 2 : 1. Between these end points, sharp isosbestic points are observed indicating sequential addition of the two phosphine ligands. No further change is observed with P : Cu ratios of greater than 2 : 1. Triphenyl phosphite gave similar results to the monophosphines with the exception that the second endpoint was poorly defined indicating weak binding of the second phosphite. With chelating phosphines, a distinct end point is observed at a ligand : copper ratio of 1 : 1. Again, sharp isosbestic points are observed indicating a clean equilibrium. At larger ligand : metal ratios the UV-spectrum returns to that of the free pyvd ligand with sharp endpoints at a 2 : 1 ligand to copper ratio for the ligands dppe and dppp. UV spectra of the phosphine complexes were obtained from the endpoints of the titrations. Representative spectra are shown in Fig. 1, while maxima and extinction coefficients are given in Table 1.

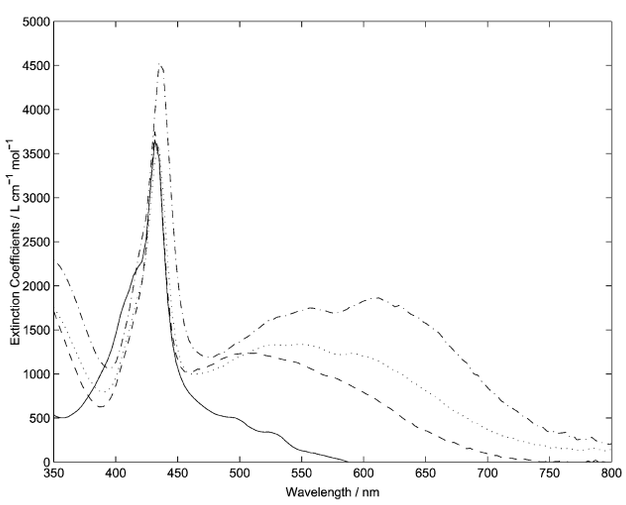

Fig. 1 UV-vis spectra of representative complexes {Cu(pyvd)[$(PhO)_3$-P]$_2$}$^+$ (—), {Cu(pyvd)([*p*-tolyl]$_3$P)$_2$}$^+$ (- - -), {Cu(pyvd)(dppb)}$^+$ (· · ·) and {Cu(pyvd)(dppp)}$^+$ (- · -).

ESR spectra were recorded on solutions of pyvd containing an excess of copper and phosphorus ligand to ensure the presence of only one ESR active species. These spectra are complex, with potentially as many as eight distinct hyperfine parameters. Nevertheless, beginning with the hyperfine parameters from the free ligand[20] and those reported by Kaim for copper–phosphine–imine radical anion complexes[21,22] acceptable simulations were obtained. An example simulation is shown in Fig. 2 and hyperfine parameters are listed in Table 2. Attempts at ENDOR spectroscopy to provide definitive resolution of the hyperfine parameters failed as a result of an inability to saturate the ESR resonance.

Table 1 UV-vis spectral details for Cu–pyvd–phosphine complexes. Wavelengths are reported in nm, extinction coefficients in L mol^{-1} cm^{-1}

Phosphine	λ_{max} (ε) π–π*	λ_{max} (ε) MLCT
None[20]	409 (1600)	450 (400) n–π*
Ph_3P	430 (3200)	498 (1100)
(*p*-tolyl)$_3$P	432 (3100)	510 (1000), 570 w sh (800)
$(PhO)_3P$	432 (2700)	490 sh (380), 520 sh (250)
dppe	438 (3500)	559 sh (1100), 612 (1200)
dppp	437 (2700)	556 sh (1000), 612 (1100)
dppb	434 (2700)	530 (1000), 550 (1000), 589 sh (940)
dppf	435 (3000)	503 (1000), 545 sh (950), 585 sh (930)
xantphos	434 (2700)	523 (1000), 547 sh (990), 585 sh (900)

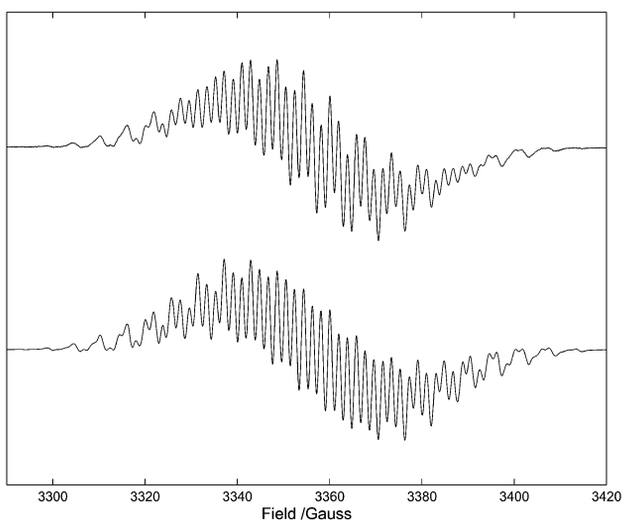

Fig. 2 X-Band ESR spectrum (top) and simulation (bottom) of {Cu(pyvd)([*p*-tolyl]$_3$P)$_2$}$^+$. Simulation parameters are given in Table 2.

Mass spectra recorded on solutions at the endpoint of titrations, and on solutions used for ESR spectroscopy, showed ions with masses corresponding to the proposed copper(I)(pyvd) bisphosphine complexes. For the titrations, with the exception of the triphenyl phosphite complex, this was the only significant ion observed. For triphenyl phosphite, masses corresponding to both $[(PhO)_3P]Cu(pyvd)^+$ and $[(PhO)_3P]_2Cu(pyvd)^+$ were observed, consistent with the observed weak coordination of the second phosphite. A representative mass spectrum is shown in Fig. 3 for the complex (pyvd)(dppf)Cu$^+$. For the solutions

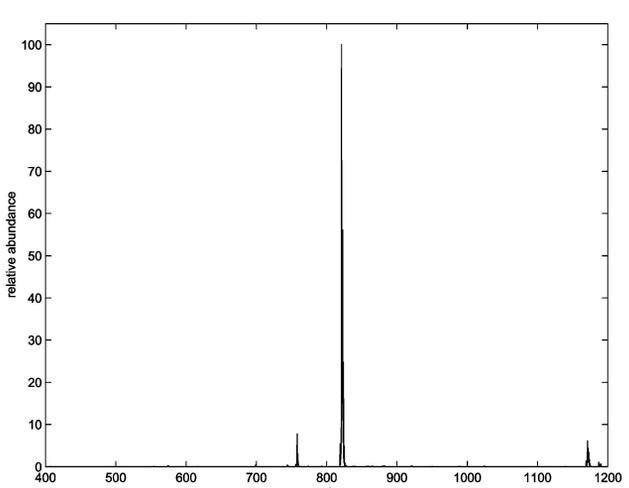

Fig. 3 Electrospray mass spectrum of the solution resulting from the reaction of pyvd with a slight excess of $Cu(MeCN)_4^+PF_6^-$ and dppf in dichloromethane. The peak at *m*/*z* = 821 corresponds to Cu(dppf)(pyvd)$^+$ while the peak at *m*/*z* = 1181 indicates a trace of $(dppf)_2Cu^+$.

Table 2 Estimated ESR hyperfine parameters for Cu–pyvd–phosphine complexes. Coupling constants for the ligand pyvd are included for comparison. Coupling constants and linewidths are reported in Gauss

Phosphine	g	a_{Cu}	a_P	a_{N2}	$a_{N1,4,5}$	a_H	Linewidth	Correlation coefficient[a]
None[20]	2.0036	–	–	6.4 (N_2,N_4)	5.4 (N_1,N_5)	5.4	0.5	
Ph_3P	2.0058	7.5	9.3	7.4	5.5	6.1	0.8	0.981
(p-tolyl)$_3$P	2.0065	7.6	9.7	7.3	5.4	6.1	0.8	0.973
$(PhO)_3P$	2.0067	9.0	12.2	7.6	5.5	6.4	1.46	0.996
dppe	2.0065	11.6	14.1	7.5	5.8	5.6	1.29	0.989
dppp	2.0068	10.0	14.3	7.3	5.7	5.6	1.49	0.995
dppb	2.0069	8.6	11.4	7.3	5.7	6.0	1.64	0.997
dppf	2.0068	8.9	11.6	7.3	5.4	6.0	0.98	0.977
xantphos	2.0071	8.6	11.1	7.3	6.0	5.8	0.6	0.897

[a] Correlation coefficient between experimental and simulated spectra.

used for ESR spectroscopy, additional peaks were observed corresponding to copper(I) phosphine species, consistent with the presence of excess phosphine and copper(I). These species are ESR silent and transparent in the visible region and thus do not affect the conclusions of this study. Despite numerous attempts, stable crystalline samples of the mixed ligand complexes could not be obtained. This may be due to ligand dissociation or ligand redistribution reactions, both common with copper(I) systems,[23] combined with the known limited stability of the pyvd radical.[20,24] Nevertheless, we feel our mass spectral data strongly supports our proposed structure for the solution species and strengthens our assignment of the spectral data.

Discussion

The UV-vis spectrum of pyvd consists of two overlapping bands that have been attributed to n–π* and π–π* bands respectively.[20] On coordination to metal ions both the intensity and wavelength of these bands increases,[3,20,25] however the change is particularly pronounced in the case of copper(I) as a result of the appearance of a metal–ligand charge transfer (MLCT) transition. In the particular systems of this study, the UV-vis spectrum shows a strong dependence on the phosphine ancillary ligand. The complexes can be divided into four groups based on the appearance of the UV-vis spectrum. The chelating ligands with the smallest bite angle, dppe and dppp, give the lowest energy MLCT band with a maximum around 610 nm and a series of shoulders and smaller maxima at higher energy. Chelating ligands with larger bite angles, dppb, dppf and xantphos, give a broad band centered near 550 nm with shoulders and additional maxima at higher and lower wavelengths. Triphenylphosphine and tri(*p*-tolyl)phosphine each give one MLCT band with a maximum near 500 nm, though a very weak shoulder may be seen in the tri(*p*-tolyl) complex near 570 nm. Triphenyl phosphite gives a spectrum similar to those observed for zinc and cadmium complexes of pyvd with a weak MLCT transition that shows some vibronic structure. Spectra representative of these four groups are plotted in Fig. 1. From this classification it appears that both geometric and electronic factors play a role in the electronic structure of these complexes; these factors may be further elucidated through examination of the ESR spectra.

Little has been reported of the ESR spectra of metal verdazyl complexes. Though parameters were reported for the complexes of Zn, Cd and Hg, little perturbation of the hyperfine structure of the ligand was seen.[20] In the remaining reported coordination compounds hyperfine coupling was not observed or the ESR spectra were not reported. In the present systems, hyperfine structure is resolved and can be simulated by assuming coupling to copper and phosphorus in addition to the nitrogens and methyl hydrogens in the verdazyl ring system. There is a significant amount of uncertainty in the simulation of these spectra as a result of the many parameters; it may be possible to find an acceptable simulation with incorrect hyperfine coupling. Unfortunately, this problem could not be resolved with ENDOR spectroscopy because we were unable to saturate the ESR resonance. Similar problems with ENDOR have been reported with other Cu(I) radical anion complexes.[21] In order to evaluate our simulations we have compared our parameters with those reported for similar systems; in particular we find the hyperfine coupling to Cu and P is consistent with other copper–phosphine radical systems. Furthermore, with the exception of the dppe complex, the Cu and P hyperfine couplings follow the empirical linear relationship described by Razuvaev:[26]

$$a_{Cu} = 3.4 + 0.44a_P$$

where a_{Cu} and a_P are hyperfine couplings to Cu and P respectively, recorded in Gauss.

The ESR parameters for the dppe complex remain slightly anomalous; though we have made repeated attempts to find simulation parameters consistent with Razuvaev's equation the parameters reported in Table 2 provide a better fit to the experimental data.

When examined as a function of ligand, the hyperfine parameters for the verdazyl ring are remarkably constant, with one coupling to nitrogen enhanced by the coordination of a metal ion. On the other hand, those for the copper and phosphine show some ligand variation. With the exception of the triphenyl phosphite system, the dependence parallels the UV-vis spectra, and hyperfine coupling to copper can be used to divide the complexes into the same four groups. The monodentate phosphines (Ph_3P and (p-tolyl)$_3$P) show the weakest copper hyperfine ($a_{Cu} \approx 7.5$ G), while the larger angle bidentate ligands (dppb, dppf, xantphos) show intermediate values for copper hyperfine ($a_{Cu} \approx 8$–9 G).[27] The small bite angle bidentate ligands (dppe and dppp) show greatest hyperfine coupling to copper ($a_{Cu} \approx 10$–12 G). The triphenyl phosphite system shows hyperfine parameters intermediate between the two groups of bidentate ligands.

Orbital overlap models have previously been used to explain the variation in spin density of copper(I) semiquinone complexes.[26,28] Though the symmetry of the verdazyl ligand differs somewhat from a semiquinone, the same considerations apply. Part of the spin density on copper arises purely from spin polarization;[26] transfer of spin density to copper can also arise from mixing of the singly occupied verdazyl π* orbital, with orbitals of appropriate (π) symmetry on the copper ion.

In the coordinate scheme of Fig. 4 these are the filled copper $3d_{xz}$ and $3d_{yz}$ orbitals and the empty copper $4p_z$ orbital. The anti-symmetric combination of phosphorus lone pairs (ϕ_P) is also of appropriate (π) symmetry to interact with the copper $3d_{yz}$ and $4p_z$ orbitals resulting in the variation of spin density and electronic transitions observed upon changing the phosphine ligand. In order to elaborate this model it is convenient to consider the copper–bis(phosphine) fragment and the verdazyl radical separately and then consider the interactions between

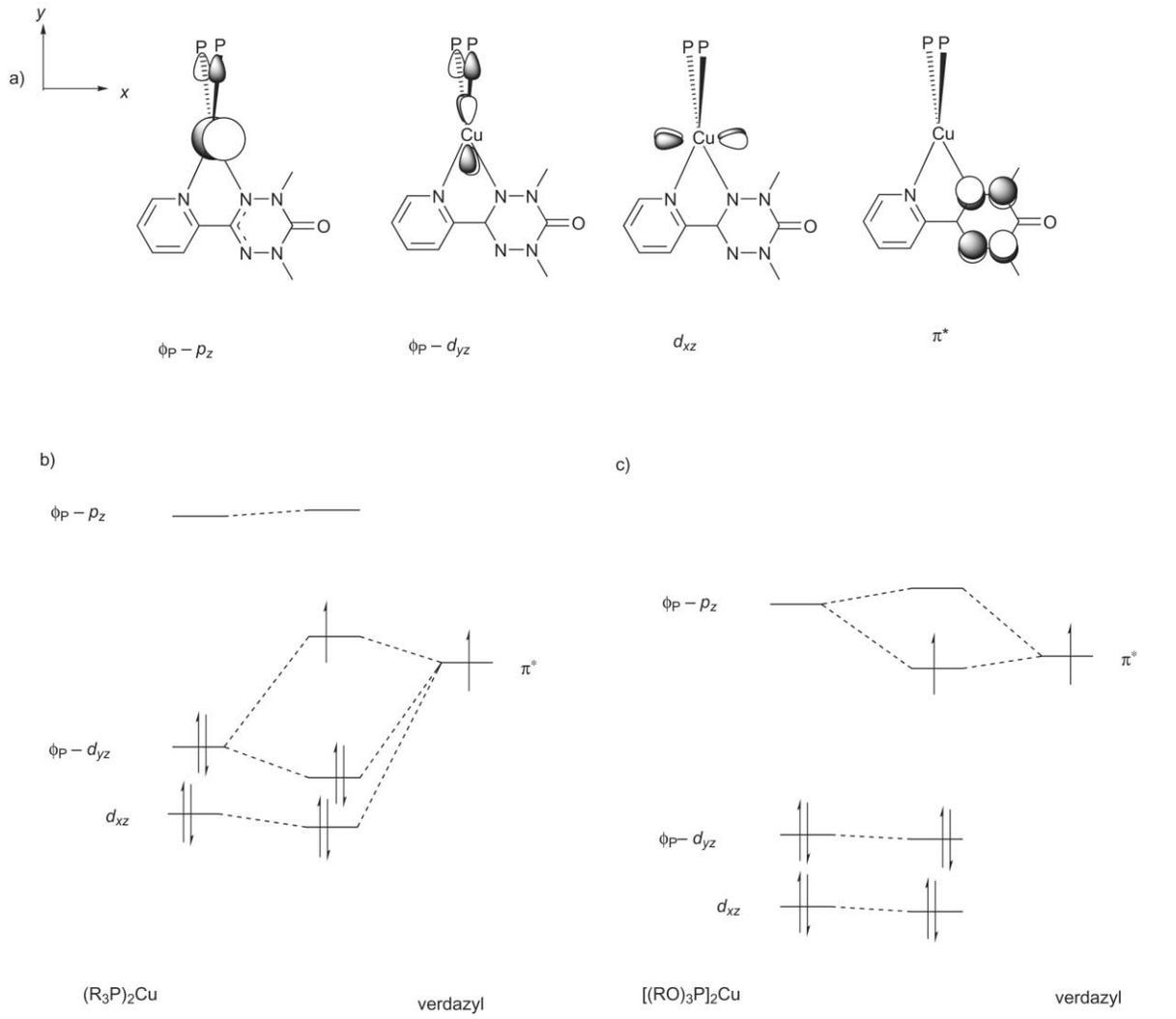

Fig. 4 Cartoon of the proposed orbital overlap scheme in copper–pyvd–phosphine complexes. a) Composite frontier orbitals for the copper–bis(phosphine) and verdazyl units. b) With phosphines, interaction of the verdazyl SOMO with the ϕ_P–$3d_{yz}$ orbital predominates. c) With weakly basic phosphite ligands, interaction with of the SOMO with the ϕ_P–$4p_z$ orbital predominates.

the two units. The antibonding combination of the phosphorus lone pairs with the copper $3d_{yz}$ orbital gives a filled metal centered orbital (ϕ_P–d_{yz}). A similar antibonding combination with the copper $4p_z$ orbital gives an empty metal centered orbital (ϕ_P–p_z). In our coordinate system the d_{xz} orbital is unaffected by the phosphorus lone pairs. The verdazyl SOMO (π^*) is delocalized over all four nitrogen atoms of the verdazyl ring. These four groups of orbitals are illustrated in Fig. 4a. When the copper–phosphine unit coordinates to the verdazyl ring, π back bonding from d_{xz} and ϕ_P–d_{yz} transfers spin density from the verdazyl ring to copper, and gives rise to the metal–ligand charge transfer band(Fig. 4b). With the chelating phosphines, the increased overlap between the phosphine and copper d orbitals raises the energy of ϕ_P–d_{yz}, increasing the spin density on copper and reducing the energy of the MLCT band. This effect is further enhanced as the ligand bite angle gets smaller (dppp and dppe).

Triphenyl phosphite is a much weaker base than the other phosphines.[29] This is reflected in the weaker coordination of the second triphenyl phosphite to the copper–verdazyl system. The decreased basicity also lowers the energy of ϕ_P–p_z and ϕ_P–d_{yz} with respect to the verdazyl SOMO, increasing the energy of the MLCT band and allowing transfer of spin density from π^* to ϕ_P–p_z (Fig. 4c). This model for the phosphite systems is supported by Razuvaev's data with triethyl phosphite complexes where coupling to the phosphorus in these systems is larger than with the corresponding phosphine.[26] The presence of d and p orbital pathways for the transfer of spin density has also been observed in metal semiquinone complexes, though in those systems different metals were associated with each pathway.[30] The ability to switch between coupling mechanisms by changing ancillary ligands may be useful in the design of magnetic materials. Competing exchange pathways may also be responsible for apparently anomalous results such as the recently reported copper(I) bis(verdazyl) system where the coupling between two radicals mediated by a copper atom was found to be close to zero.[16] Studies in progress will examine other copper(I) verdazyl systems in order to further examine this issue.

Conclusion

The electronic and ESR spectra of copper(I) verdazyl phosphine complexes show a pronounced variation depending on the geometric and electronic properties of the ancillary phosphine ligand. Small bite angle chelating ligands and to a lesser extent, strongly donating ligands give a greater spin density on copper, while weakly donating ligands can also increase spin density on copper through a different mechanism. These variations in spin density may be useful in the control of magnetism in extended verdazyl systems.

Acknowledgements

We would like to thank Dr S. Schlick for use of her ESR spectrometer. Funding for this research was provided by the

Petroleum Research Fund, Grant 35178-GB3,1 to D. J. R. B., and the National Science Foundation, Award CHE-0116181 for purchase of an LC/MS system.

References

1 D. J. R. Brook, S. Fornell, B. Noll, G. Yee and T. H. Koch, *J. Chem. Soc., Dalton Trans.*, 2000, 2019.
2 D. J. R. Brook, B. Conklin, V. Lynch and M. A. Fox, *J. Am. Chem. Soc.*, 1997, **119**, 5155.
3 R. G. Hicks, M. T. Lemaire, L. K. Thompson and T. M. Barclay, *J. Am. Chem. Soc.*, 2000, **122**, 8077.
4 T. M. Barclay, R. G. Hicks, M. T. Lemaire and L. K. Thompson, *Chem. Commun.*, 2000, 2141.
5 P. Baxter, J.-M. Lehn, A. DeCian and J. Fischer, *Angew. Chem., Int. Ed. Engl.*, 1993, **32**, 69.
6 J.-M. Lehn, A. Rigault, J. Siegel, J. Harrowfield, B. Chevrier and D. Moras, *Proc. Natl. Acad. Sci. USA*, 1987, **84**, 2565.
7 J.-M. Lehn and A. Rigault, *Angew. Chem., Int. Ed. Engl.*, 1988, **27**, 1095.
8 U. Ziener, E. Breuning, J.-M. Lehn, E. Wegelius, K. Rissanen, G. Baum, D. Fenske and G. Vaughan, *Chem. Eur. J.*, 2000, **6**, 4132.
9 J. Rojo, F. J. Romero-Salguero, J.-M. Lehn, G. Baum and D. Fenske, *Eur. J. Inorg. Chem.*, 1999, 1421.
10 G. S. Hanan, D. Volkner, U. S. Schubert, J.-M. Lehn, G. Baum. and D. Fenske, *Angew. Chem., Int. Ed. Engl.*, 1997, **37**, 1842.
11 G. S. Hanan, C. R. Arana, J.-M. Lehn, G. Baum and D. Fenske, *Chem. Eur. J.*, 1996, **2**, 1292.
12 A. M. Garcia, F. J. Romero-Salguuero, D. M. Bassani, J.-M. Lehn, G. Baum and D. Fenske, *Chem. Eur. J.*, 1999, **5**, 1803.
13 A. M. Garcia, D. M. Bassani, J.-M. Lehn, G. Baum and D. Fenske, *Chem. Eur. J.*, 1999, **5**, 1234.
14 P. Ceroni, A. Credi, V. Balzani, S. Campagna, G. S. Hanan, C. R. Arana and J.-M. Lehn, *Eur. J. Inorg. Chem.*, 1999, 1409.
15 M. T. Green and T. A. McCormick, *Inorg. Chem.*, 1999, **38**, 3061.
16 T. M. Barclay, R. G. Hicks, M. T. Lemaire and L. K. Thompson, *Inorg. Chem.*, 2001, **40**, 6521.
17 M. Kranenburg, Y. E. M. van der Burgt, P. C. J. Kamer and P. W. N. M. van Leeuwen, *Organometallics*, 1995, **14**, 3081.
18 D. R. Duling, *J. Magn. Reson., Ser. B*, 1994, **104**, 105.
19 MATLAB 6.0.0.88, The MathWorks Inc., 3 Apple Hill Drive, Natick, MA, USA, 2000.
20 D. J. R. Brook, S. Fornell, J. E. Stevens, B. Noll, T. H. Koch and W. Eisfeld, *Inorg. Chem.*, 2000, **39**, 562.
21 M. Glöckle, K. Hübler, H.-J. Kümmerer, G. Denninger and W. Kaim, *Inorg. Chem.*, 2001, **40**, 2263.
22 A.-L. Barra, L.-C. Brunel, F. Baumann, M. Schwach, M. Moscherosch and W. Kaim, *J. Chem Soc., Dalton Trans.*, 1999, 3855.
23 J. R. Kirchhoff, D. R. McMillin, W. R. Robinson, D. R. Powell, A. T. McKenzie and S. Chen, *Inorg. Chem.*, 1985, **24**, 3928.
24 C. L. Barr, P. A. Chase, R. G. Hicks, M. T. Lemaire and C. L. Stevens, *J. Org. Chem.*, 1999, **64**, 8388.
25 T. M. Barclay, R. G. Hicks, M. T. Lemaire and L. K. Thompson, *Inorg. Chem.*, 2001, **40**, 5581.
26 G. A. Razuvaev, V. K. Cherkasov and G. A. Abakumov, *J. Organomet. Chem.*, 1978, **160**, 361.
27 P. W. N. M. van Leeuwen, P. C. J. Kamer, J. N. H. Reek and P. Dierkes, *Chem. Rev.*, 2000, **100**, 2741.
28 A. Rockenbauer, M. Gyor, G. Speier and Z. Tyeklar, *Inorg. Chem.*, 1987, **26**, 3293.
29 F. A. Cotton and G. Wilkinson, *Advanced Inorganic Chemistry*, Wiley, New York, 1988.
30 C. G. Pierpont and C. W. Lange, *Prog. Inorg. Chem.*, 1994, **41**, 331.